



Public Health
England



NHS Breast Screening Programme Equipment Report

Technical Evaluation of Hologic 3Dimensions digital mammography system in 2D mode

March 2019

About Public Health England

Public Health England exists to protect and improve the nation's health and wellbeing, and reduce health inequalities. We do this through world-leading science, knowledge and intelligence, advocacy, partnerships and the delivery of specialist public health services. We are an executive agency of the Department of Health and Social Care, and a distinct delivery organisation with operational autonomy. We provide government, local government, the NHS, Parliament, industry and the public with evidence-based professional, scientific and delivery expertise and support.

Public Health England, Wellington House, 133-155 Waterloo Road, London SE1 8UG

Tel: 020 7654 8000 www.gov.uk/phe

Twitter: [@PHE_uk](https://twitter.com/PHE_uk) Facebook: www.facebook.com/PublicHealthEngland

About PHE screening

Screening identifies apparently healthy people who may be at increased risk of a disease or condition, enabling earlier treatment or informed decisions. National population screening programmes are implemented in the NHS on the advice of the UK National Screening Committee (UK NSC), which makes independent, evidence-based recommendations to ministers in the 4 UK countries. PHE advises the government and the NHS so England has safe, high quality screening programmes that reflect the best available evidence and the UK NSC recommendations. PHE also develops standards and provides specific services that help the local NHS implement and run screening services consistently across the country.

www.gov.uk/phe/screening Twitter: [@PHE_Screening](https://twitter.com/PHE_Screening) Blog: phescreening.blog.gov.uk

For queries relating to this document, please contact: phe.screeninghelpdesk@nhs.net

Prepared by: A Mackenzie, JM Oduko

© Crown copyright 2019

You may re-use this information (excluding logos) free of charge in any format or medium, under the terms of the Open Government Licence v3.0. To view this licence, visit [OGL](https://www.ogil.io/) or email psi@nationalarchives.gsi.gov.uk. Where we have identified any third party copyright information you will need to obtain permission from the copyright holders concerned.

Published March 2019

PHE publications

gateway number: GW-264

PHE supports the UN

Sustainable Development Goals



Contents

About Public Health England	2
About PHE screening	2
Executive summary	4
1. Introduction	5
1.1 Testing procedures and performance standards for digital mammography	5
1.2 Objectives	5
2. Methods	5
2.1 System tested	5
2.2 Output and half value layer	6
2.3 Detector response	7
2.4 Dose measurement	8
2.5 Contrast-to-noise ratio	8
2.6 AEC performance for local dense areas	10
2.7 Noise analysis	11
2.8 Image quality measurements	12
2.9 Physical measurements of the detector performance	14
2.10 Other tests	14
3. Results	15
3.1 X-ray tube output and half value layer	15
3.2 Detector response	15
3.3 Automatic exposure control performance	16
3.4 Noise measurements	19
3.5 Image quality measurements	21
3.6 Comparison with other systems	23
3.7 Detector performance	27
3.8 Other tests	29
3.9 Curved paddle	30
4. Discussion	33
5. Conclusions	35
References	36

Executive summary

The purpose of the evaluation was to determine whether the Hologic 3Dimensions, operating in 2D mode, meets the main standards in the NHS Breast Screening Programme (NHSBSP) and European protocols, and to provide performance data for comparison against other systems.

The MGD was found to be well below the remedial level. For a 53mm equivalent standard breast, the MGD was 1.37mGy using Auto-Filter AEC mode, compared with the remedial level of 2.5mGy. The image quality, as measured by threshold gold thickness, was better than the achievable level.

The Hologic 3Dimensions meets the requirements of the NHSBSP standards for digital mammography systems operating in 2D mode.

1. Introduction

1.1 Testing procedures and performance standards for digital mammography

This report is one of a series evaluating commercially available direct digital radiography (DR) systems for mammography on behalf of the NHS Breast Screening Programme (NHSBSP). The testing methods and standards applied are mainly derived from NHSBSP Equipment Report 0604¹ which is referred to in this document as ‘the NHSBSP protocol’. The standards for image quality and dose are the same as those provided in the European protocol,^{2,3} but the latter has been followed where it provides a more detailed standard, for example, for the automatic exposure control (AEC) system.

Some additional tests were carried out according to the UK recommendations for testing mammographic X-ray equipment as described in IPEM Report 89.⁴

1.2 Objectives

The aims of the evaluation were:

- to determine whether the Hologic 3Dimensions digital mammography system, operating in 2D mode, meets the main standards in the NHSBSP and European protocols
- to provide performance data for comparison against other systems

2. Methods

2.1 System tested

The tests were conducted at the Hologic factory, Danbury, CT, USA, on a Hologic 3Dimensions system as described in Table 1. Some additional measurements were made at the Jarvis Breast Screening Unit, Guildford, UK on the curved compression paddle. The Hologic 3Dimensions is shown in Figure 1.

Table 1. System description

Manufacturer	Hologic Inc
Model	3Dimensions
System serial number	PROTO 7
Target material	Tungsten (W)
Added filtration	50µm Rhodium (Rh), 50µm Silver (Ag), [700µm Aluminium (Al) used for tomosynthesis]
Detector type	Amorphous selenium
Detector serial number	YM868282
Pixel size	70µm
Detector size	240mm x 300mm
Pixel array	2560 x 3328, 3328 x 4096
Typical image sizes	16MB (18x24cm field size), 27MB (24x29cm field size)
Pixel value offset	50
Source to detector distance	700mm
Source to table distance	675mm
Pre-exposure mAs	5mAs for compressed breast thickness (CBT) ≤50mm; 10mAs for CBT >50mm
Automatic exposure control modes	Auto-Filter, Auto-kV, Auto-Time
Software version	1.9.0.632

There is a choice of 2 types of breast compression paddles: standard flat paddles and curved paddles. All tests were undertaken using flat paddles apart from section 3.10.

2.2 Output and half value layer

The output and half-value-layer (HVL) were measured as described in the NHSBSP protocol, at intervals of 3kV. The kV was measured with a RMI 232 kV meter, which had been calibrated for exposures using a W/Rh target/filter combination.

Figure 1. The Hologic 3Dimensions



2.3 Detector response

The detector response was measured as described in the NHSBSP protocol, except that 2mm aluminium was used at the tubehead, instead of PMMA. The grid was removed and an ion chamber was positioned above the breast support table, 40mm from the chest wall edge (CWE). The incident air kerma was measured for a range of manually set mAs values at 29kV W/Rh. The readings were corrected to the surface of the detector using the inverse square law. No correction was made for attenuation by the detector cover. Images acquired at the same range of mAs values were saved as unprocessed files. A 10mm square region of interest (ROI) was positioned on the midline, 40mm from the CWE of each image. The average pixel value and the standard deviation of pixel values within that region were measured. The relationship between average pixel values and the detector entrance surface air kerma was determined.

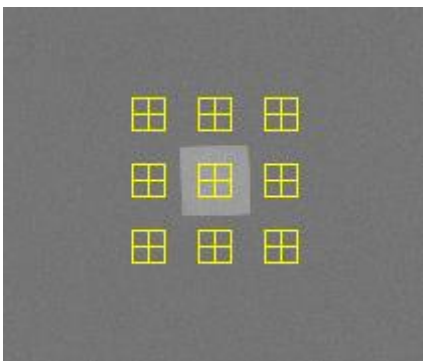
2.4 Dose measurement

Doses were measured using the X-ray set's AEC in the Auto-Filter mode to expose different thicknesses of PMMA. Each PMMA block had an area of 180mm x 240mm. Spacers were used to adjust The paddle height was adjusted to be equal to the equivalent breast thickness, as shown in Table 3. The exposure factors were noted and mean glandular doses (MGDs) were calculated for equivalent breast thicknesses. An aluminium square, 10mm x 10mm and 0.2mm thick, was used with the PMMA during these exposures, so that the images produced could be used for the calculation of the contrast-to-noise ratio (CNR), described in Section 2.5. The aluminium square was placed between 2 10mm thick slabs of 180mm x 240mm PMMA, on the midline, with its centre 60mm from the CWE. Additional layers of PMMA were placed on top to vary the total thickness.

2.5 Contrast-to-noise ratio

Unprocessed images acquired during the dose measurement were downloaded and analysed to calculate the CNRs. Thirty-six small square ROIs (approximately 2.5mm x 2.5mm) were used to determine the average signal and the standard deviation in the signal within the image of the aluminium square (4 ROIs) and the surrounding background (32 ROIs), as shown in Figure 2. Small ROIs are used to minimise distortions due to the heel effect and other causes of non-uniformity.⁵ The CNR was calculated for each image, as defined in the NHSBSP protocol.

Figure 2. Location and size of ROI used to determine the CNR



To apply the standards in the European protocol, it is necessary to relate the image quality measured using the CDMAM (Section 2.8) for an equivalent breast thickness of 60mm, to that for other breast thicknesses. The European protocol² gives the relationship between threshold contrast and CNR measurements, enabling the calculation of a target CNR value for a particular level of image quality. This can be compared to CNR measurements made at other breast thicknesses. Contrast for a

particular gold thickness is calculated using Equation 1, and target CNR is calculated using Equation 2.

$$\text{Contrast} = 1 - e^{-\mu t} \quad (1)$$

where μ is the effective attenuation coefficient for gold, and t is the gold thickness.

$$\text{CNR}_{\text{target}} = \frac{\text{CNR}_{\text{measured}} \times \text{TC}_{\text{measured}}}{\text{TC}_{\text{target}}} \quad (2)$$

where $\text{CNR}_{\text{measured}}$ is the CNR for a 60mm equivalent breast, $\text{TC}_{\text{measured}}$ is the threshold contrast calculated using the threshold gold thickness for a 0.1mm diameter detail, (measured using the CDMAM at the same dose as used for $\text{CNR}_{\text{measured}}$), and $\text{TC}_{\text{target}}$ is the calculated threshold contrast corresponding to the threshold gold thickness required to meet either the minimum acceptable or achievable level of image quality as defined in the UK standard.

The threshold gold thickness of the 0.1mm diameter detail is used here because it is generally regarded as the most critical of the detail diameters for which performance standards are set.

The effective attenuation coefficient for gold used in Equation 1 depends on the beam quality used for the exposure, and the value used is in Table 2. These values were calculated with 3mm PMMA representing the compression paddle, using spectra from Boone et al.⁶ and attenuation coefficients for materials in the test objects (aluminium, gold, PMMA) from Berger et al.⁷

The European protocol also defines a limiting value for CNR, which is calculated as a percentage of the threshold contrast for minimum acceptable image quality for each thickness. This limiting value varies with thickness, as shown in Table 3.

Table 2. Effective attenuation coefficients for gold contrast details in the CDMAM

kV	Target/filter	Effective attenuation coefficient (μm^{-1})
31	W/Rh	0.120

Table 3. Limiting values for relative CNR

Thickness of PMMA (mm)	Equivalent breast thickness (mm)	Limiting values for relative CNR (%) in European protocol
20	21	> 115
30	32	> 110
40	45	> 105

45	53	> 103
50	60	> 100
60	75	> 95
70	90	> 90

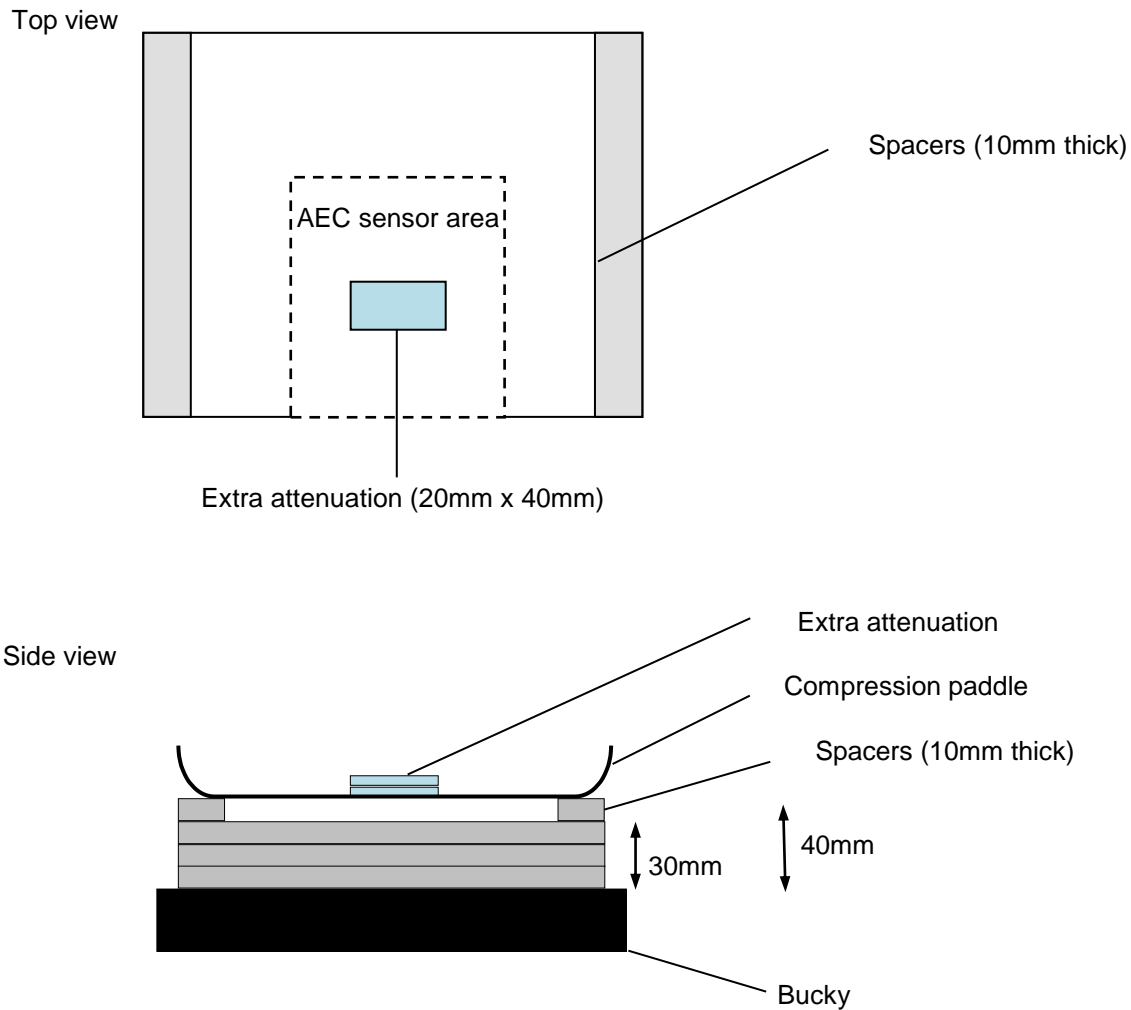
The target CNR values for minimum acceptable and achievable levels of image quality and European limiting values for CNR were calculated. These were compared with the measured CNR results for all breast thicknesses.

2.6 AEC performance for local dense areas

This test is described in the supplement to the fourth edition of the European protocol.³ To simulate local dense areas, images of a 30mm thick block of PMMA of size 180mm x 240mm, were acquired under AEC. Extra PMMA between 2 and 20mm thick and of size 20mm x 40mm was added to provide extra attenuation. The compression plate remained in position at a height of 40mm, as shown in Figure 3. The simulated dense area was positioned 50mm from the CWE of the table.

In the simulated local dense area the mean pixel value and standard deviation for a 10mm x 10mm ROI were measured and the signal-to-noise ratios (SNRs) were calculated.

Figure 3. Setup to measure AEC performance for local dense areas



2.7 Noise analysis

The images acquired in the measurements of detector response, using 29kV W/Rh, were used to analyse the image noise. Small ROIs with an area of approximately 2.5mm x 2.5mm were placed on the midline, 60mm from the CWE. The average standard deviations of the pixel values in these ROIs for each image were used to investigate the relationship between the dose to the detector and the image noise. It was assumed that this noise comprises 3 components: electronic noise, structural noise, and quantum noise. The relationship between them is shown in Equation 3:

$$\sigma_p = \sqrt{k_e^2 + k_q^2 p + k_s^2 p^2} \quad (3)$$

where σ_p is the standard deviation in pixel values within an ROI with a uniform exposure and a mean pixel value p , and k_e , k_q , and k_s are the coefficients determining the

amount of electronic, quantum, and structural noise in a pixel with a value p . This method of analysis has been described previously.⁸ For simplicity, the noise is generally presented here as relative noise defined as in Equation 4.

$$\text{Relative noise} = \frac{\sigma_p}{p} \quad (4)$$

The variation in relative noise with mean pixel value was evaluated and fitted using Equation 3, and non-linear regression used to determine the best fit for the constants and their asymptotic confidence limits (using Graphpad Prism version 7.00, Graphpad software, San Diego, California, USA, www.graphpad.com). This established whether the experimental measurements of the noise fitted this equation, and the relative proportions of the different noise components. The relationship between noise and pixel values has been found empirically to be approximated by a simple power relationship as shown in Equation 5.

$$\frac{\sigma_p}{p} = k_t p^{-n} \quad (5)$$

where k_t is a constant. If the noise were purely quantum noise the value of n would be 0.5. However the presence of electronic and structural noise means that n can be slightly higher or lower than 0.5.

The variance in pixel values within a ROI is defined as the standard deviation squared. The total variance was plotted against incident air kerma at the detector.

Using the calculated constants, the structural, electronic, and quantum components of the variance were estimated, assuming that each component was independently related to incident air kerma. The percentage of the total variance represented by each component was then calculated and plotted against incident air kerma at the detector.

2.8 Image quality measurements

Contrast detail measurements were made using a CDMAM phantom (serial number 1022, version 3.4, UMC St. Radboud, Nijmegen University, Netherlands). The phantom was positioned with a 20mm thickness of PMMA above and below, to give a total attenuation approximately equivalent to 50mm of PMMA or 60mm thickness of typical breast tissue. The exposure factors were chosen to be close to those selected by the AEC, in Auto-Filter mode, when imaging a 50mm thickness of PMMA. This procedure was repeated to obtain a representative sample of 16 images at this dose level. The unprocessed images were transferred to disk for subsequent analysis off-site. Further sets of 16 images of the test phantom were then obtained at other dose levels by manually selecting higher and lower mAs values with the same beam quality. The CDMAM images were read and analysed automatically using Version 1.6 of CDCOM.^{9,10} and Version 2.1.0 of CDMAM Analysis (www.nccpm.org). The threshold gold thickness for a typical human observer was predicted using Equation 6.

$$TC_{\text{predicted}} = rTC_{\text{auto}} \quad (6)$$

where $TC_{\text{predicted}}$ is the predicted threshold contrast for a typical observer, TC_{auto} is the threshold contrast measured using an automated procedure with CDMAM images. r is the average ratio between human and automatic threshold contrast determined experimentally with the values shown in Table 4.

Table 4. Values of r used to predict threshold contrast

Diameter of gold disc (mm)	Average ratio of human to automatically measured threshold contrast (r)
0.08	1.40
0.10	1.50
0.13	1.60
0.16	1.68
0.20	1.75
0.25	1.82
0.31	1.88
0.40	1.94
0.50	1.98
0.63	2.01
0.80	2.06
1.00	2.11

The predicted threshold gold thickness for each detail diameter in the range 0.1mm to 1.0mm was fitted with a curve for each dose level, using the relationship shown in Equation 7.

$$\text{Threshold gold thickness} = a + bx^{-1} + cx^{-2} + dx^{-3} \quad (7)$$

where x is the detail diameter, and a , b , c and d are coefficients adjusted to obtain a least squares fit.

The confidence limits for the predicted threshold gold thicknesses have been previously determined by a sampling method using a large set of images. The threshold contrasts quoted in the tables of results are derived from the fitted curves, as this has been found to improve accuracy.

The expected relationship between threshold contrast and dose is shown in Equation 8.

$$\text{Threshold contrast} = \lambda D^{-n} \quad (8)$$

where D is the MGD for a 60mm thick standard breast (equivalent to the test phantom configuration used for the image quality measurement), and λ is a constant to be fitted.

It is assumed that a similar equation applies when using threshold gold thickness instead of contrast. This equation was plotted with the experimental data for detail diameters of 0.1 and 0.25mm. The value of n resulting in the best fit to the experimental data was determined, and the doses required for target CNR values were calculated for data relating to these detail diameters.

2.9 Physical measurements of the detector performance

The modulation transfer function (MTF), normalised noise power spectrum (NNPS) and the detective quantum efficiency (DQE) of the system were measured. The methods used were as close as possible to those described by the International Electrotechnical Commission (IEC).¹¹ The radiation quality used for the measurements was adjusted by placing a uniform 2mm thick aluminium filter at the tube housing. The beam quality used was 29kV W/Rh. The test device to measure the MTF comprised of a 120mm x 60mm rectangle of stainless steel with polished straight edges, of thickness 0.8mm. This test device was placed directly on the breast support table, and the grid was removed by selecting “grid out” at the operator console. The test device was positioned to measure the MTF in 2 directions, first almost perpendicular to the CWE and then almost parallel to it. The MTF was then calculated, including MTF50%, which is the spatial frequency at which the MTF is equal to 0.5,

To measure the noise power spectrum the test device was removed and exposures made for a range of incident air kerma at the surface of the table, where around 75 μ Gy was used as the mid-dose value. The DQE is presented as the average of measurements in the directions perpendicular and parallel to the CWE.

2.10 Other tests

Other tests were carried out to cover the range that would normally form part of a commissioning survey on new equipment. These included tests prescribed in IPEM Report 89⁴ for mammographic X-ray sets, as well as those in the UK NHSBSP protocol for digital mammographic systems. The tests measured tube voltage, accuracy of indicated compressed breast thickness, alignment of radiation field to light field and image, image retention, focal spot dimensions, AEC reproducibility, image uniformity, cycle time and backup timer.

3. Results

3.1 X-ray tube output and half value layer

The HVL and tube output measurements are shown in Table 5.

Table 5. HVL and tube output measurement

kV	HVL (mm Al)		Output ($\mu\text{Gy/mAs}$ at 1m)	
	W/Rh	W/Ag	W/Rh	W/Ag
25	0.48	-	10.1	-
28	0.51	0.54	14.0	18.1
31	0.54	0.57	17.9	23.6
34	0.56	0.60	21.8	29.0
37	0.58	0.63	25.5	34.5

The tube voltage measurements are shown in Table 6. All were within 1.0kV of indicated values and are within the IPEM Report 89⁴ remedial level of $\pm 1\text{kV}$.

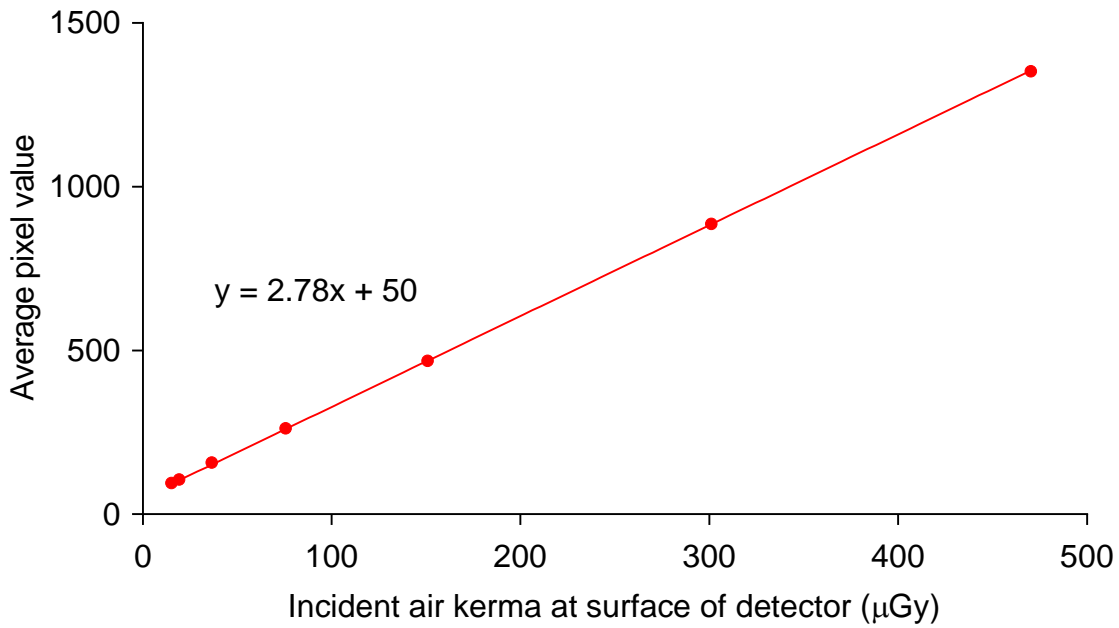
Table 6. kV measurements made with W/Rh target/filter combination

kV set	kV measured
25	26.0
28	28.6
31	30.9
34	33.9

3.2 Detector response

The detector response is shown in Figure 4. Measurements were made using 29kV W/Rh.

Figure 4. Detector response



3.3 Automatic exposure control performance

3.3.1 Dose

The MGDs for breasts simulated with PMMA, exposed using AEC, are shown in Figure 5 and Table 7.

Figure 5 MGD for different thicknesses of simulated breasts under AEC. (Error bars indicate 95% confidence limits.)

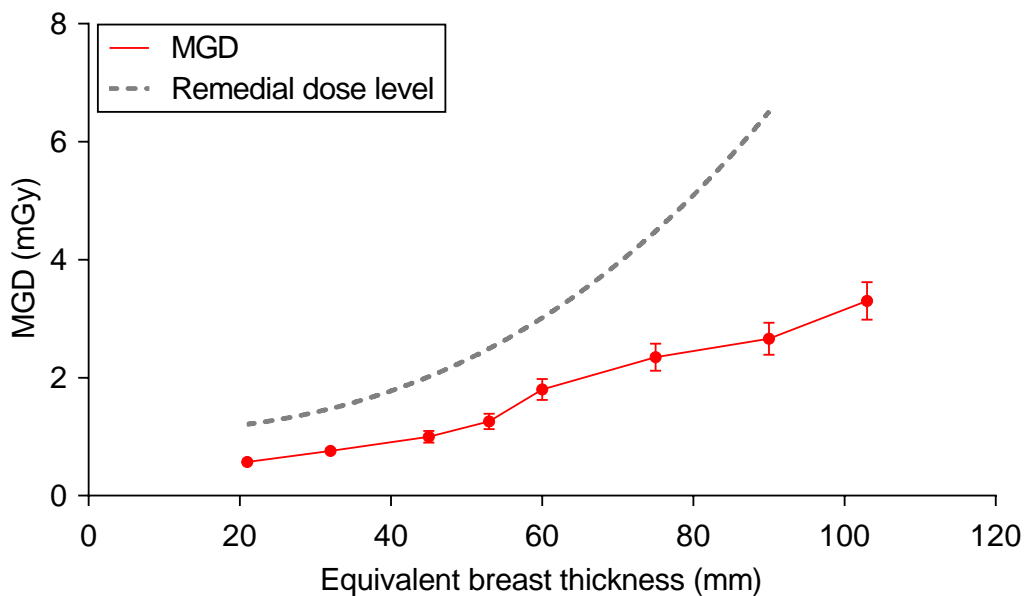


Table 7. MGD for simulated breasts, AEC Auto-Filter mode

PMMA thickness (mm)	Equivalent breast thickness (mm)	kV	Target/filter	mAs	MGD (mGy)	Remedial dose level (mGy)	Displayed dose (mGy)
20	21	25	W/Rh	50	0.57	1.0	0.58
30	32	26	W/Rh	73	0.76	1.5	0.75
40	45	28	W/Rh	92	1.00	2.0	1.00
45	53	29	W/Rh	113	1.26	2.5	1.24
50	60	31	W/Rh	142	1.80	3.0	1.75
60	75	31	W/Ag	151	2.35	4.5	2.24
70	90	34	W/Ag	151	2.66	6.5	2.63
80	103	36	W/Ag	173	3.30	-	3.73

The difference between the displayed doses and the calculated MGDs was within 5% for equivalent breast thicknesses, except for 103mm equivalent breast thickness where the displayed MGD was 17% higher.

3.3.2 Contrast-to-Noise ratio

The results of the CNR measurements are shown in Figure 6 and Table 8. The following calculated values are also shown:

- CNR to meet the minimum acceptable image quality standard at the 60mm breast thickness
- CNR to meet the achievable image quality standard at the 60mm breast thickness
- CNRs at each thickness to meet the limiting value in the European protocol

Figure 6. CNR for 0.2mm Al measured in the Auto Filter mode. (Error bars indicate 95% confidence limits.)

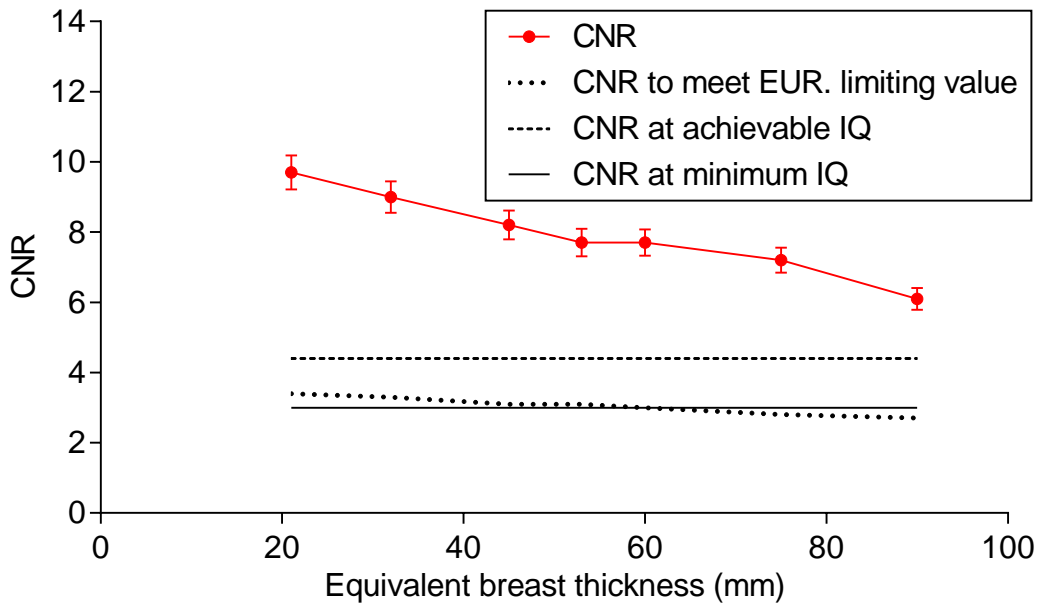


Table 8. CNR measurements, exposures under AEC(Auto-Filter)

PMMA thickness (mm)	Equivalent breast thickness (mm)	Measured CNR	CNR for minimum acceptable IQ	CNR for achievable IQ	European limiting CNR value
20	21	9.7	3.0	4.4	3.4
30	32	9.0	3.0	4.4	3.3
40	45	8.2	3.0	4.4	3.1
45	53	7.7	3.0	4.4	3.1
50	60	7.7	3.0	4.4	3.0
60	75	7.2	3.0	4.4	2.8
70	90	6.1	3.0	4.4	2.7

3.3.3 AEC performance for local dense areas

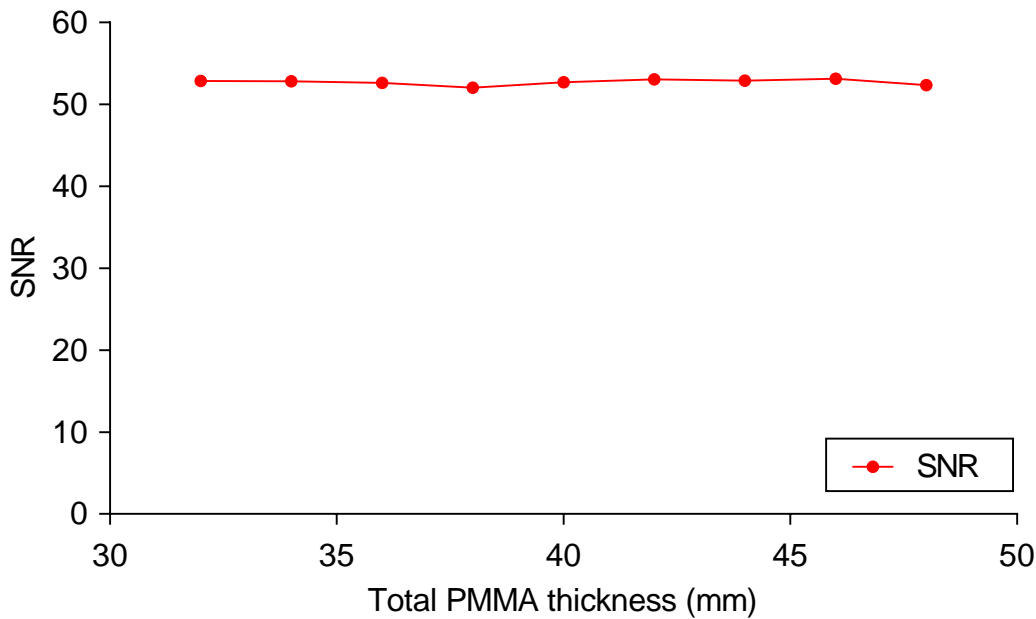
For many systems, when the AEC adjusts for locally dense areas, the SNR remains constant with increasing thickness of extra PMMA. The results of this test are shown in Table 9 and Figure 7.

The mean SNR results for different thicknesses of PMMA was 52.7. The variation in the SNR across the thicknesses of PMMA, was much smaller than the tolerance of 20%.

Table 9. AEC performance for local dense areas

Total attenuation (mm PMMA)	kV	Target/filter	Tube load (mAs)	SNR	% difference from mean SNR result
32	28	W/Rh	62	52.9	0.3%
34	28	W/Rh	68	52.8	0.2%
36	28	W/Rh	76	52.6	-0.2%
38	28	W/Rh	83	52.1	-1.3%
40	28	W/Rh	90	52.7	0.0%
42	28	W/Rh	105	53.1	0.6%
44	28	W/Rh	116	52.9	0.4%
46	28	W/Rh	126	53.1	0.8%
48	28	W/Rh	139	52.4	-0.7%

Figure 7. AEC performance for local dense area test



3.4 Noise measurements

The variation in noise with dose was analysed by plotting the standard deviation in pixel values against the incident air kerma to the detector, as shown in Figure 8. The fitted power curve has an index of 0.47, which is close to the expected value (0.5) for quantum noise sources alone.

Figure 8. Standard deviation of pixel values versus air kerma at detector

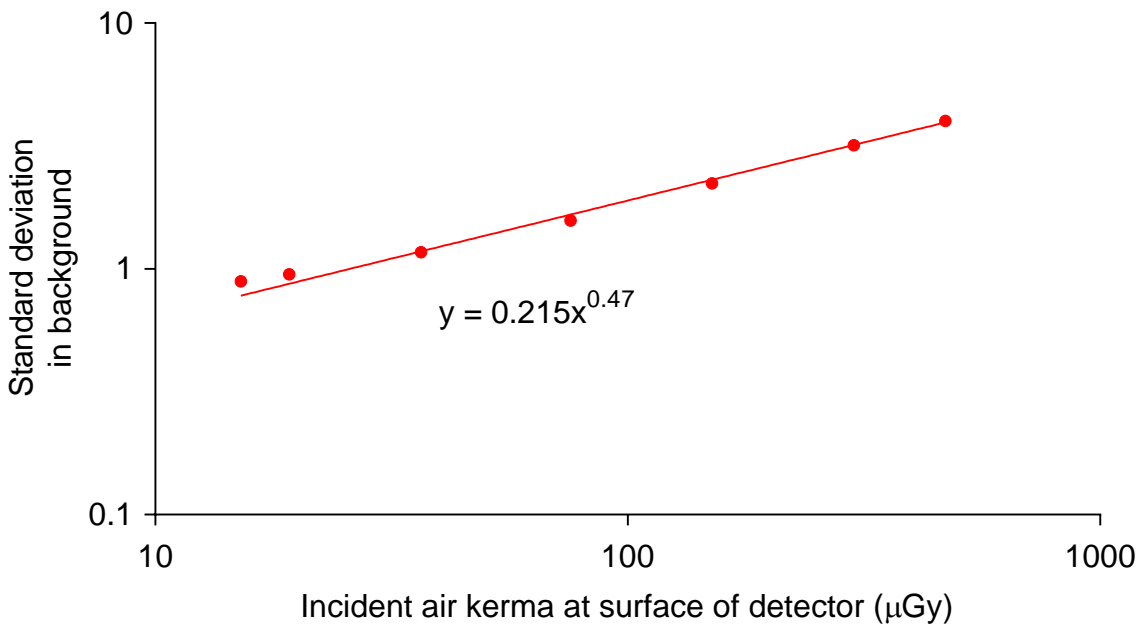


Figure 9. Relative noise and noise components

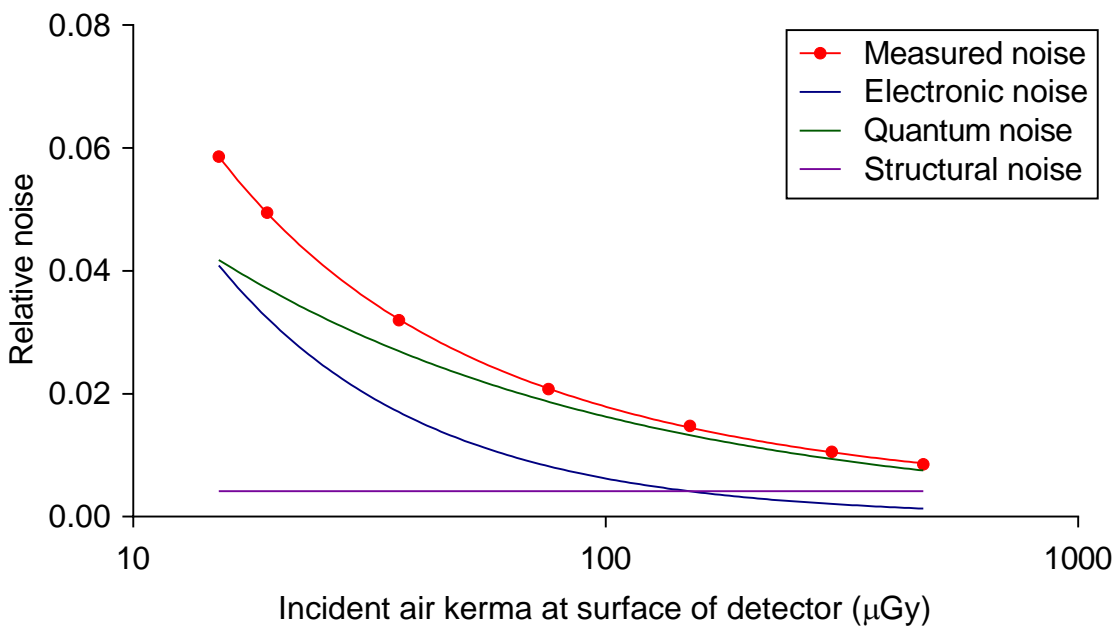
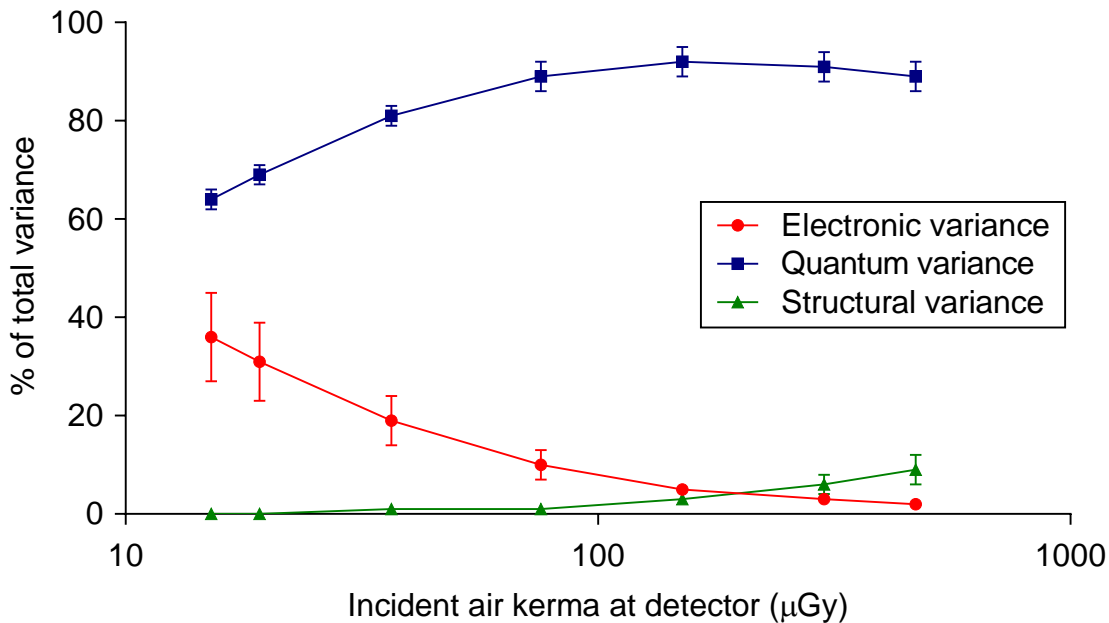


Figure 9 shows the relative noise at different entrance air kerma. The estimated relative contributions of electronic, structural, and quantum noise are shown and the quadratic sum of these contributions fitted to the measured noise (using Equation 3). The quantum component dominates over the whole range.

Figure 10 shows the different amounts of variance due to each noise component. From this, the dose range over which the quantum component dominates can be seen.

Figure 10. Noise components as a percentage of the total variance. (Error bars indicate 95% confidence limits.)



3.5 Image quality measurements

The exposure factors used for each set of 16 CDMAM images are shown in Table 10. The mAs used approximate the value selected by the AEC and double and half that value for exposures of a 60mm thick equivalent breast.

Table 10. Images acquired for image quality measurement

kV	Target/filter	Tube loading (mAs)	MGD to equivalent breasts 60mm thick (mGy)
31	W/Rh	71	0.90
31	W/Rh	140	1.77
31	W/Rh	280	3.54

The contrast detail curves (determined by automatic reading of the images) at the different dose levels are shown in Figure 11. The threshold gold thicknesses measured for different detail diameters at the 3 selected dose levels are shown in Table 11. The NHSBSP minimum acceptable and achievable limits are also shown.

The measured threshold gold thicknesses are plotted against the MGD for an equivalent breast of 60mm for the 0.1mm and 0.25mm detail sizes in Figure 12.

Figure 11. Contrast detail curves for 3 doses at 31kV W/Rh. (Error bars indicate 95% confidence limits.)

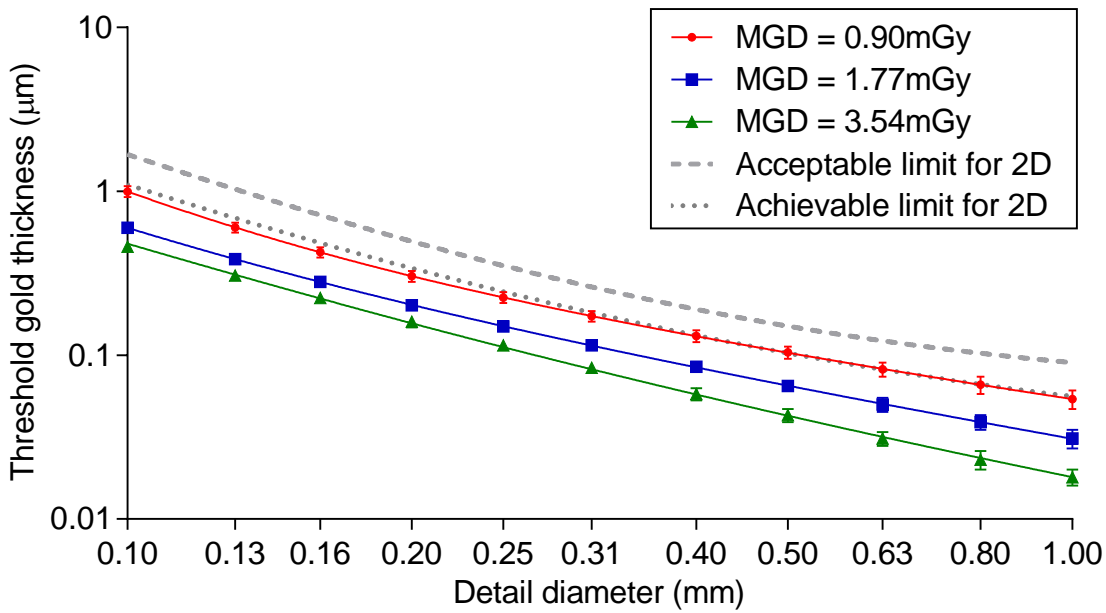
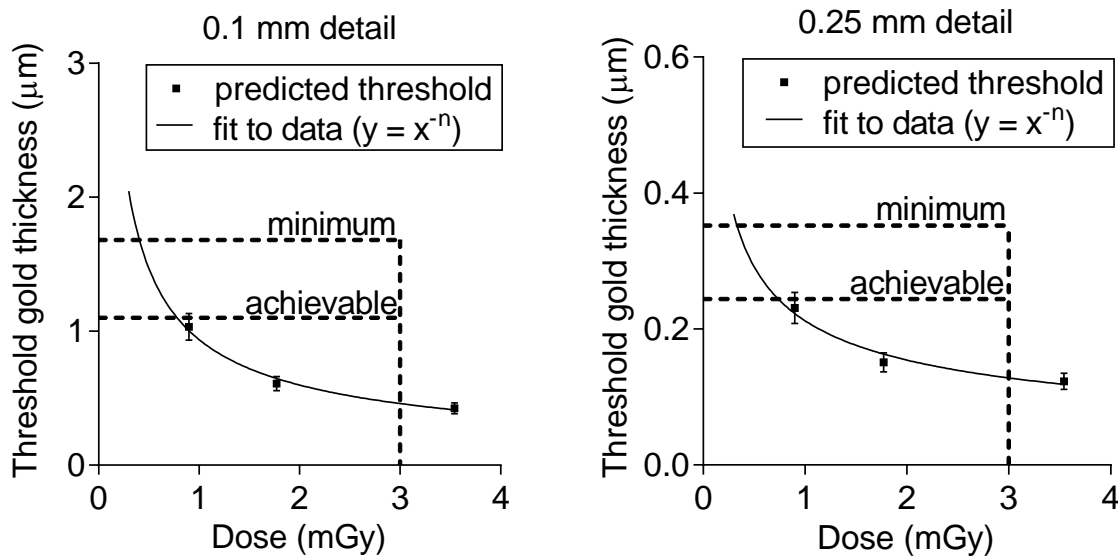


Table 11. Average threshold gold thicknesses for different detail diameters for 3 doses using 31kV W/Rh, and automatically predicted data

Detail diameter (mm)	Threshold gold thickness (µm)				
	Acceptable value	Achievable value	MGD = 0.90mGy	MGD = 1.77mGy	MGD = 3.54mGy
0.1	1.680	1.100	0.998±0.077	0.600±0.041	0.460±0.034
0.25	0.352	0.244	0.225±0.017	0.150±0.010	0.115±0.008
0.5	0.150	0.103	0.104±0.009	0.065±0.005	0.043±0.004
1.0	0.091	0.056	0.054±0.007	0.031±0.004	0.018±0.002

Figure 12. Threshold gold thickness at different doses. (Error bars indicate 95% confidence limits.)



3.6 Comparison with other systems

The MGDs to reach the minimum and achievable image quality standards in the NHSBSP protocol have been estimated from the curves shown in Figure 12. The fitted curves are of the form $y = x^{-n}$. (The error in estimating these doses depends on the accuracy of the curve fitting procedure, and pooled data for several systems has been used to estimate the 95% confidence limits of about 20%.) These doses are shown against similar data for different models of digital mammography systems in Tables 13 and 14 and Figures 13 to 16. The data for these systems has been determined in the same way as described in this report and the results published previously.¹³⁻¹⁸ The data for film-screen represents an average value determined using a variety of film-screen systems in use prior to their discontinuation.

Table 13. The MGD for a 60mm equivalent breast for different systems to reach the minimum threshold gold thickness for 0.1mm and 0.25mm details

System	MGD (mGy) for 0.1mm	MGD (mGy) for 0.25mm
GE Essential	0.49 ± 0.10	0.49 ± 0.10
Fujifilm Innovality	0.61 ± 0.12	0.49 ± 0.10
Hologic 3Dimensions	0.40 ± 0.08	0.33 ± 0.07
Hologic Dimensions (v1.4.2)	0.34 ± 0.07	0.48 ± 0.10
IMS Giotto 3DL	0.93 ± 0.19	0.70 ± 0.14
Philips MicroDose L30 C120	0.67 ± 0.13	0.47 ± 0.09
Siemens Inspiration	0.76 ± 0.15	0.60 ± 0.12
Film-screen	1.30 ± 0.26	1.36 ± 0.27
Fuji Profect CR	1.78 ± 0.36	1.35 ± 0.27

Table 14. The MGD for a 60mm equivalent breast for different systems to reach the achievable threshold gold thickness for 0.1mm and 0.25mm details

System	MGD (mGy) for 0.1mm	MGD (mGy) for 0.25mm
GE Essential	1.13 ± 0.13	1.03 ± 0.21
Fujifilm Innovality	1.15 ± 0.23	1.02 ± 0.20
Hologic 3Dimensions	0.78±0.16	0.74 ±0.15
Hologic Dimensions (v1.4.2)	0.87 ± 0.17	1.10 ± 0.22
IMS Giotto 3DL	1.60 ± 0.32	1.41 ± 0.28
Philips MicroDose L30 C120	1.34 ± 0.27	1.06 ± 0.21
Siemens Inspiration	1.27 ± 0.25	1.16 ± 0.23
Film-screen	3.03 ± 0.61	2.83 ± 0.57
Fuji Profect CR	3.29 ± 0.66	2.65 ± 0.53

Figure 13. MGD for a 60mm equivalent breast to reach minimum acceptable image quality standard for 0.1mm detail. (Error bars indicate 95% confidence limits.)

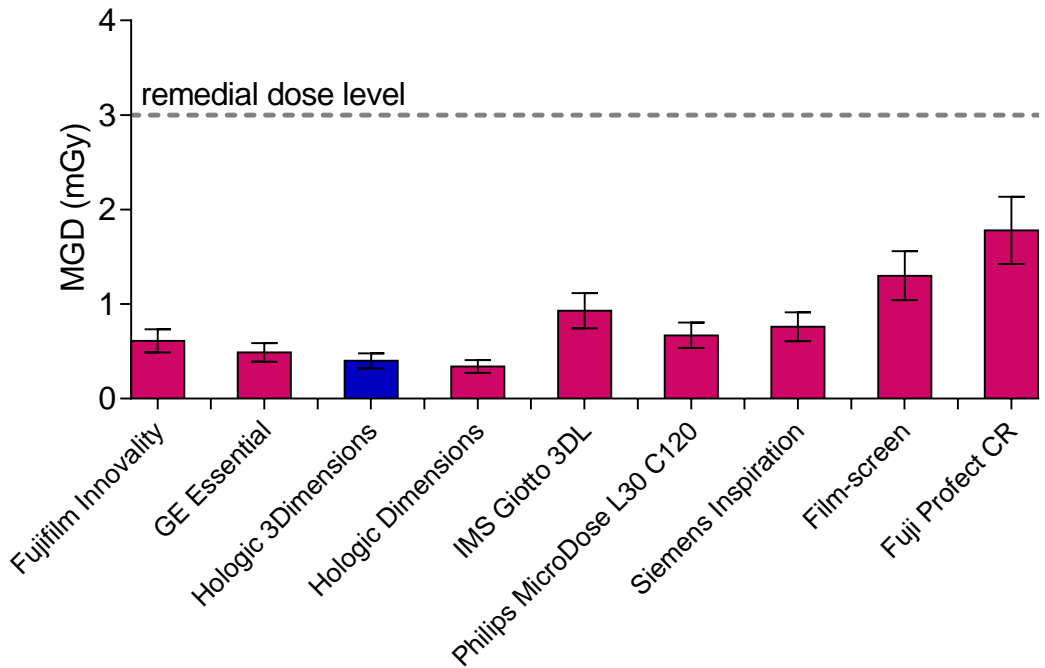


Figure 14. MGD for a 60mm equivalent breast to reach achievable image quality standard for 0.1mm detail. (Error bars indicate 95% confidence limits.)

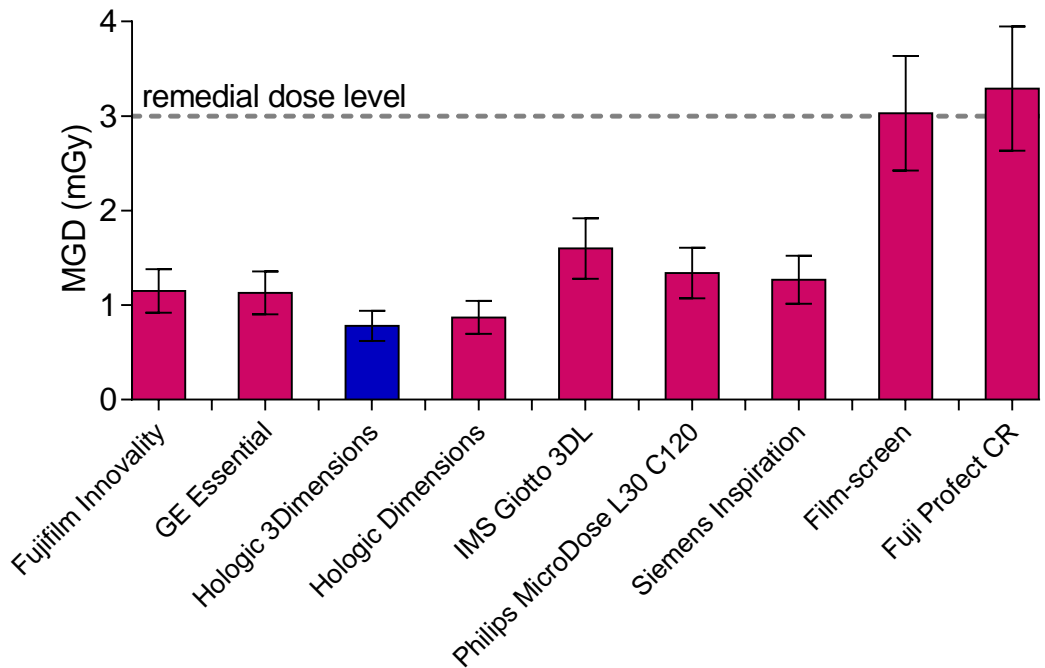


Figure 15. MGD for a 60mm equivalent breast to reach minimum acceptable image quality standard for 0.25mm detail. (Error bars indicate 95% confidence limits.)

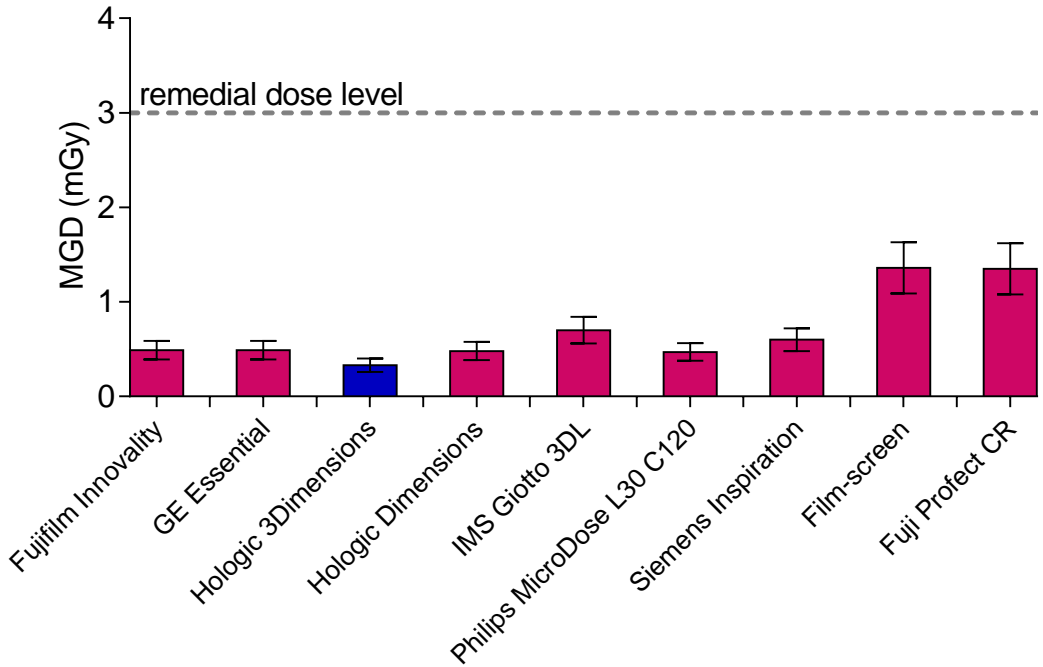
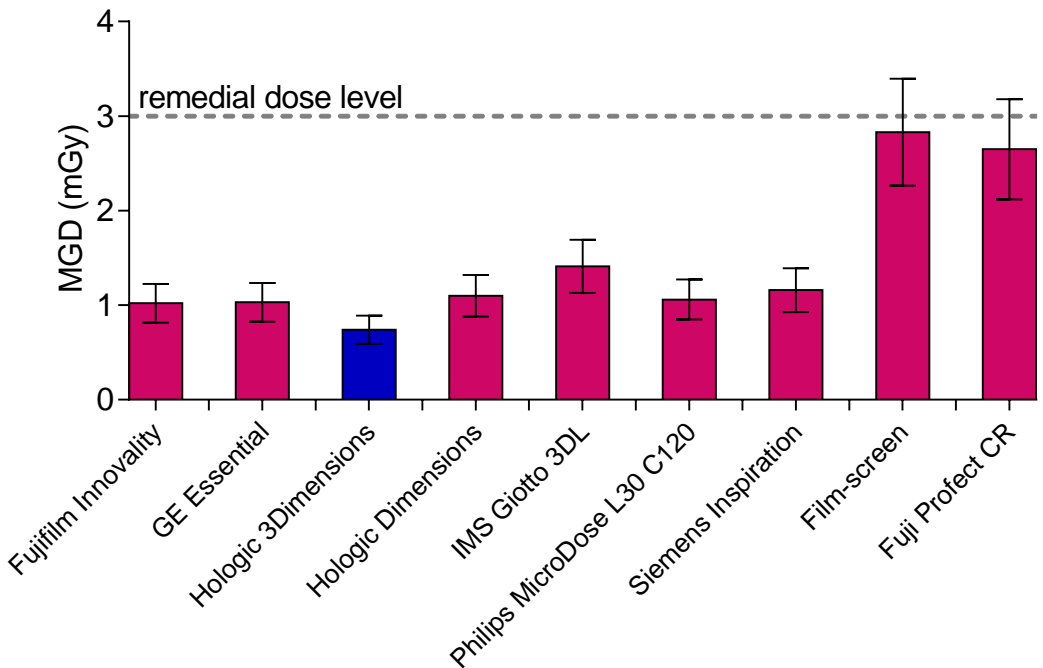


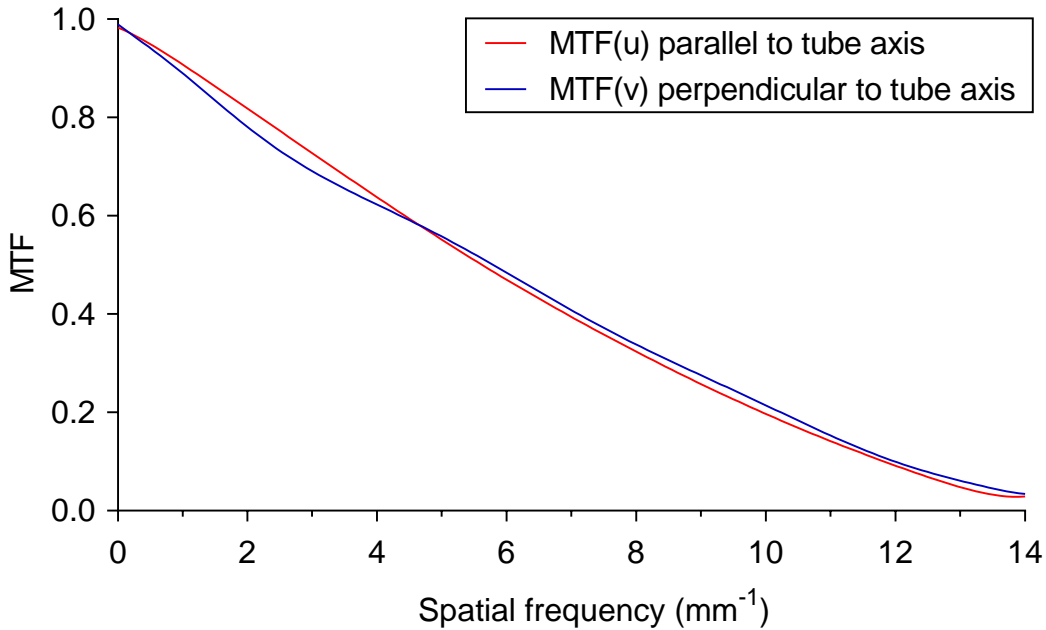
Figure 16. MGD for a 60mm equivalent breast to reach achievable image quality standard for 0.25mm detail. (Error bars indicate 95% confidence limits.)



3.7 Detector performance

The MTF is shown in Figure 17 for the 2 orthogonal directions. Figure 18 shows the NNPS curves for a range of entrance air kerma.

Figure 17. Pre-sampling MTF



The MTF50% are 5.6mm^{-1} and 5.8mm^{-1} for the u and v axes respectively.

Figure 18. NNPS curves for a range of incident air kerma to the detector

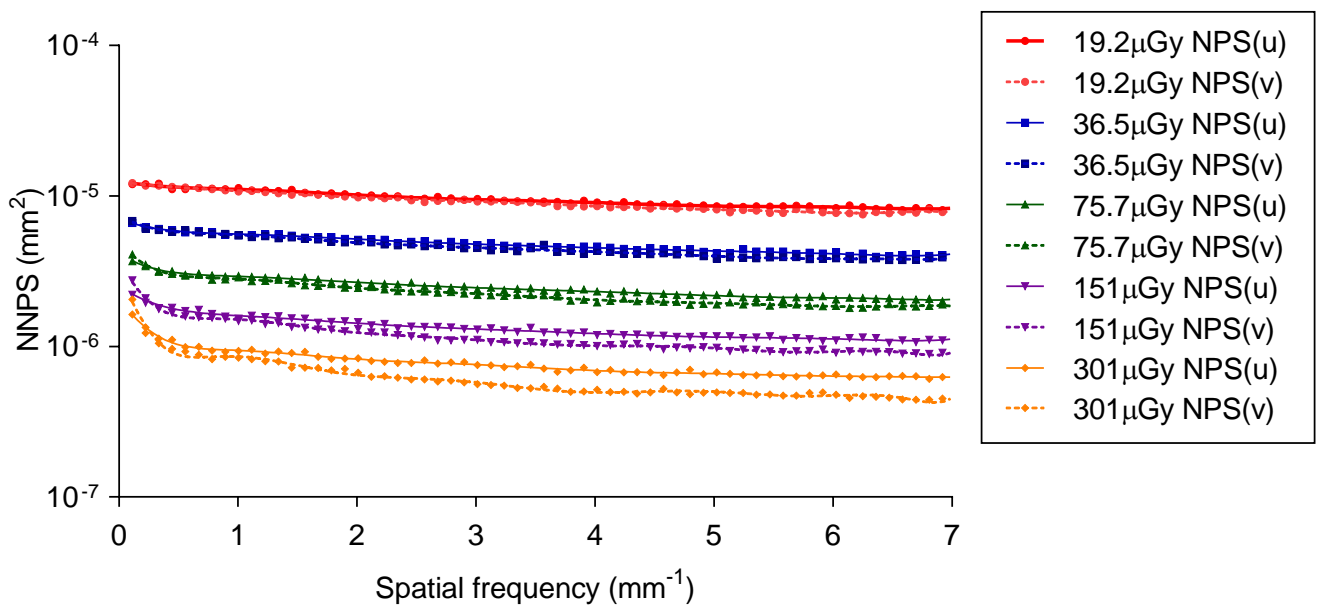


Figure 19 shows the DQE averaged in the 2 orthogonal directions for a range of incident air kerma to the detector. The MTF and DQE measurements were interpolated to show values at standard frequencies in Table 15.

Figure 19. DQE averaged in both directions for a range of incident air kerma to the detector

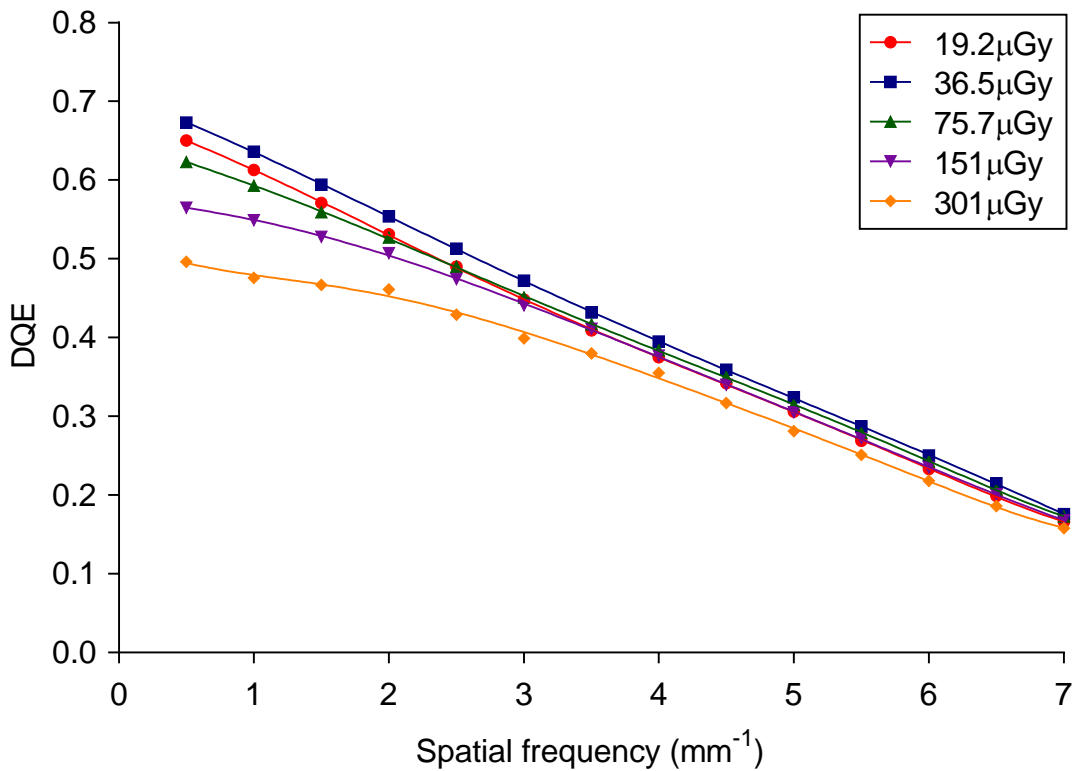


Table 15. Average of orthogonal directions of MTF and DQE measurements at spatial frequencies up to the Nyquist frequency (DQE at incident air kerma of 75.7 μGy)

Frequency (mm ⁻¹)	MTF	DQE
0.0	1.00	-
0.5	0.95	0.62
1.0	0.90	0.59
1.5	0.85	0.56
2.0	0.80	0.53
2.5	0.75	0.49
3.0	0.71	0.45
3.5	0.67	0.42
4.0	0.63	0.38
4.5	0.59	0.35
5.0	0.55	0.31

5.5	0.52	0.28
6.0	0.48	0.24
6.5	0.44	0.21
7.0	0.40	0.17

3.8 Other tests

The results of all the other tests that were carried out were within acceptable limits as prescribed in the NHSBSP protocol¹ and IPEM Report 89.⁴

3.8.1 Compression

The measured compressed breast thicknesses are compared with the displayed values in Table 16. There were no differences between the displayed and indicated values. This is well within the IPEM Report 89⁴ remedial level of > 5mm.

Table 16. Indicated compressed breast thickness

Actual thickness (mm)	Indicated thickness (mm)	Difference (mm)
20	20	0
40	40	0
70	70	0

3.8.2 Alignment

Alignment measurements for the 240mm x 300mm and 180mm x 240mm (central, left and right shift positions) field sizes showed that the light field edges were all within 5mm of the edges of the radiation field (IPEM remedial level > 5mm). The radiation field overlapped the edges of the image by up to 4.5mm (remedial level < 0mm or > 5mm) at the CWE.

3.8.3 Image retention

The image retention factor was 0.02, compared to the NHSBSP upper limit of 0.3.

3.8.4 Focal spot

The measured dimensions of the focal spot were 0.6mm x 0.4mm.

3.8.5 Mesh

No discontinuities or blurred regions were seen in the image of the mesh test object.

3.8.6 AEC repeatability

For a series of 5 repeat images, acquired in quick succession, the maximum deviation of mAs from the mean was 1.3%. For 8 images, acquired at intervals over several days of testing, the maximum deviation was 3.1%. The NHSBSP remedial level is 5%.

3.8.7 Uniformity and artefacts

Uniformity measurements showed a variation in linearised pixel values of less than 1% relative to the central area. The NHSBSP remedial level is 10%.

3.8.8 Cycle time

For a typical exposure of 29kV W/Ag at 113mAs, a subsequent exposure could be made 28 seconds after the start of the previous one.

3.8.9 Backup timer

When an AEC exposure was attempted with a steel plate blocking the X-ray beam, the exposure terminated after a short time of less than a second following the pre-exposure. There was no main exposure and no image was acquired.

3.9 Curved paddle

Hologic have introduced a curved compression paddle (SmartCurve™) for this system. The paddle is designed to more closely resemble the shape of the breast. There are 2 paddle sizes available: 18cm x 24cm and 24cm x 29cm.

The heights between the highest and lowest point of the paddle are 16mm and 23mm for the small and large paddles respectively.

Information from Hologic is that the system calculates the MGD for breasts assuming that the compressed thickness is the height of the base of the 18x24cm paddle plus 8mm, which represents the average breast thickness averaged over the entire curved surface of the paddle.

It was not possible to test the AEC function using the standard size blocks of PMMA, as it was not possible to position the paddle at the required height due to its curvature. The required thickness of PMMA was therefore assembled using blocks of different sizes as shown in Figure 10.

Figure 20. 18cm x24cm curved paddle with PMMA

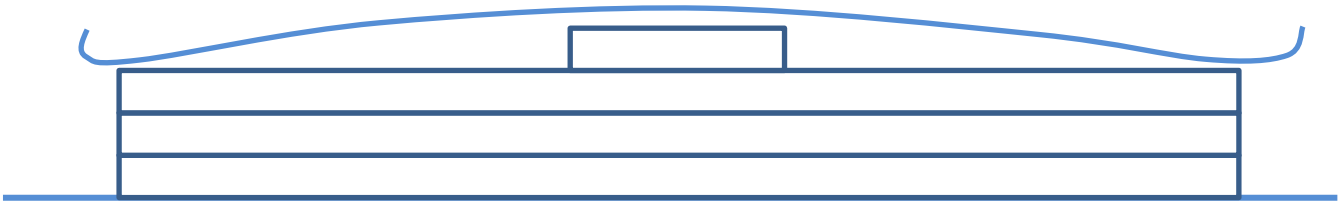


Table 17. Exposure factors and displayed MGD for simulated breasts using flat paddle (18cm x 24cm) and curved paddles (18cm x 24cm and 24cm x 29cm), exposures acquired using AEC

PMMA thickness (mm)	Displayed breast thickness (mm)	kV	Target/filter	Flat 18cm x 24cm		Curved 18cm x 24cm		Curved 24cm x 29cm	
				mAs	MGD (mGy)	mAs	MGD (mGy)	mAs	MGD (mGy)
20	21	25	W/Rh	58	1.29	59	0.66	59	0.67
30	32	26	W/Rh	86	0.87	83	0.86	87	0.90
40	45	28	W/Rh	109	1.19	109	1.20	113	1.24
45	53	29	W/Rh	130	1.49	126	1.45	128	1.47
50	60	31	W/Rh	162	2.13	165	2.16	163	2.14
60	75	31	W/Ag	183	2.95	179	2.87	179	2.88
70	90	34	W/Ag	182	3.52	179	3.46	179	3.45

4. Discussion

The detector response was found to be linear with a pixel value offset of 50. This was as expected for Hologic systems.

MGDs measured using PMMA were well within the NHSBSP limits for all equivalent breast thicknesses (Figure 5). The MGD to a 53mm equivalent breast thickness was 1.26mGy (Table 7). The displayed doses were very close to the calculated MGDs, except for 103mm equivalent breast thickness.

CNR measurements made with plain PMMA showed a steady decrease with increasing equivalent breast thickness. The target CNR values of 3.0 and 4.4, for minimum acceptable and achievable image quality respectively, were calculated from the CNR and threshold gold thickness results. All CNR values exceeded the European limiting values for CNR (Table 8).

The European guidelines³ state that system should adjust the exposures in response to the thickness of added PMMA. A provisional tolerance of is that the SNR is kept within 20% of the average SNR. The results (Table 9) showed a minimal change in SNR for the different thicknesses of PMMA.

Noise analysis showed that quantum noise dominates the noise over a wide range of incident air kerma (Figure 10). The noise variance associated with electronic noise reached 38% of the total noise variance at very low incident air kerma.

Threshold gold thicknesses for a range of detail diameters are shown in Figure 11. At a dose level (MGD = 1.77mGy) approximately that for a 60mm thick equivalent breast , the image quality was better than the achievable level for all contrast detail diameters.

Threshold gold thickness measurements at different dose levels for the 0.1mm and 0.25mm diameter details were used to calculate MGDs (to a simulated 60mm equivalent breast) required for the minimum and achievable levels of image quality (Figure 12). This allowed comparisons to be made between this and other systems previously tested. The dose required for the 3Dimensions to reach the achievable level of image quality was relatively low to that calculated for other digital mammography systems (Tables 13-14).

The detector performance, as indicated by MTF, NNPS and DQE curves (Figures 17-19), was satisfactory.

The miscellaneous results presented under the Section 3.9 “Other tests” were satisfactory.

In addition to the standard flat paddle, this system has 2 curved paddles. For the same displayed compressed breast thickness and thickness in the X-ray beam usig each of

the paddles, then the system chose very similar radiographic factors and displayed similar MGDs. Though it should be noted that the current dose model is based on a flat paddle.

5. Conclusions

The MGD of 1.26mGy for a breast thickness of 53mm is below the remedial dose level. The image quality, as measured by threshold gold thickness, is better than the achievable level.

The Hologic 3Dimensions meets the requirements of the NHBSP standards for 2D digital mammography systems.

References

1. Kulama E, Burch A, Castellano I et al. *Commissioning and routine testing of full field digital mammography systems* (NHSBSP Equipment Report 0604, Version 3). Sheffield: NHS Cancer Screening Programmes, 2009
2. van Engen R, Young KC, Bosmans H, et al. European protocol for the quality control of the physical and technical aspects of mammography screening. In *European guidelines for quality assurance in breast cancer screening and diagnosis*, Fourth Edition. Luxembourg: European Commission, 2006
3. van Engen R, Bosmans H, Dance D et al. Digital mammography update: European protocol for the quality control of the physical and technical aspects of mammography screening. In *European guidelines for quality assurance in breast cancer screening and diagnosis*, Fourth edition – Supplements. Luxembourg: European Commission, 2013
4. Moore AC, Dance DR, Evans DS et al. *The Commissioning and Routine Testing of Mammographic X-ray Systems*. York: Institute of Physics and Engineering in Medicine, Report 89, 2005
5. Alsager A, Young KC, Oduko JM. Impact of heel effect and ROI size on the determination of contrast-to-noise ratio for digital mammography systems. In *Proceedings of SPIE Medical Imaging*, Bellingham WA: SPIE Publications, 2008, 691341: 1-11
6. Boone JM, Fewell TR and Jennings RJ. Molybdenum, rhodium and tungsten anode spectral models using interpolating polynomials with application to mammography *Medical Physics*, 1997, 24: 1863-1974
7. Berger MJ, Hubbell JH, Seltzer SM, Chang et al. XCOM: Photon Cross Section Database (version 1.3) <http://physics.nist.gov/xcom> (Gaithersburg, MD, National Institute of Standards and Technology), 2005
8. Young KC, Oduko JM, Bosmans H, Nijs K, Martinez L. Optimal beam quality selection in digital mammography. *Brit. J. Radiol.*, 2006, 79: 981-990
9. Young KC, Cook JH, Oduko JM. Automated and human determination of threshold contrast for digital mammography systems. In *Proceedings of the 8th International Workshop on Digital Mammography*, Berlin: Springer-Verlag, 2006, 4046: 266-272
10. Young KC, Alsager A, Oduko JM et al. Evaluation of software for reading images of the CDMAM test object to assess digital mammography systems. In *Proceedings of SPIE Medical Imaging*, Bellingham WA: SPIE Publications, 2008, 69131C: 1-11

11. IEC 62220-1-2, *Determination of the detective quantum efficiency – Detectors used in mammography*. International Electrotechnical Commission, 2007
12. Young KC, Cook JJH, Oduko JM. Use of the European protocol to optimise a digital mammography system. In *Proceedings of the 8th International Workshop on Digital Mammography*, Berlin, Germany: Springer-Verlag, Lecture Notes in Computer Science, 2006, 4046:362-369
13. Young KC, Oduko JM. *Technical evaluation of the Hologic Selenia full field digital mammography system with a tungsten tube* (NHSBSP Equipment Report 0801). Sheffield: NHS Cancer Screening Programmes, 2008
14. Young KC, Oduko JM, Gundogdu O and Asad M. *Technical evaluation of profile automatic exposure control software on GE Essential FFDM systems* (NHSBSP Equipment Report 0903). Sheffield: NHS Cancer Screening Programmes, 2009
15. Young KC, Oduko JM, Gundogdu, O, Alsager, A. *Technical evaluation of Siemens Mammomat Inspiration Full Field Digital Mammography System* (NHSBSP Equipment Report 0909). Sheffield: NHS Cancer Screening Programmes, 2009
16. Young KC, Oduko JM. *Technical evaluation of Hologic Selenia Dimensions 2-D Digital Breast Imaging System with software version 1.4.2* (NHSBSP Equipment Report 1201). Sheffield: NHS Cancer Screening Programmes, 2012
17. Oduko JM, Young KC. *Technical evaluation of Philips MicroDose L30 with AEC software version 8.3* (NHSBSP Equipment Report 1305). Sheffield: NHS Cancer Screening Programmes, 2013
18. Strudley CS, Oduko JM, Young KC. *Technical evaluation of the Fujifilm Amulet Innovality Digital Mammography System* (NHSBSP Equipment Report 1601). London, Public Health England, 2017